Chemical Engineering Journal 472 (2023) 144938

Contents lists available at ScienceDirect

Chemical Engineering Journal

journal homepage: www.elsevier.com/locate/cej

# Natural sediments activating peroxydisulfate for *in situ* degradation of antibiotics under anoxic conditions: The critical role of surface-adsorbed and structural Fe(II)

Wenjuan Liao [a,b,c], Wei Peng [a], Peng Liao [b,*], Yanqi Xiao [a], Wenjing Xie [d], Ao Qian [d,e], Yaqi Ning [a], Na Zhang [c], Elias Niyuhire [f], Hao-Jie Cui [a,*]

[a] College of Resources, Hunan Agricultural University, Changsha 410128, PR China
[b] State Key Laboratory of Environmental Geochemistry, Institute of Geochemistry, Chinese Academy of Sciences, Guiyang 550081, PR China
[c] Hebei Key Laboratory of Wetland Ecology and Conservation, Hengshui University, Hengshui 053000, PR China
[d] School of Environment and Health, Jianghan University, Wuhan 430056, PR China
[e] State Key Laboratory of Biogeology and Environmental Geology, China University of Geosciences, Wuhan 430078, PR China
[f] Ecole Normale Supérieure, Département des Sciences Naturelles, Centre de Recherche en Sciences et de Perfectionnement Professionnel, Boulevard Mwezi Gisabo, BP: 6983 Bujumbura, Burundi

ARTICLE INFO

*Keywords:*
Fe(II) species
Anoxic sediments
Peroxydisulfate activation
Sulfamethoxazole degradation
Mechanisms

ABSTRACT

Peroxydisulfate (PDS) is widely used in groundwater remediation systems. Previous studies investigated its activation by natural sediments under oxic conditions. However, the role of sediments Fe(II) species in PDS activation under anoxic conditions remains unclear. This work elucidated the activation of PDS and concurrent degradation of sulfamethoxazole (SMX) in sediments-based systems under various anoxic scenarios. The reaction of 10 g/L sediment suspensions with 2.2 mM PDS degraded SMX (10 μM) up to 86.4%, leading to the decrease of SMX toxicity towards *Photobacterium phoshoreum T3 spp*. PDS activation by solid Fe(II) species in the sediments generated sulfate ($SO_4^{\bullet-}$), hydroxyl (•OH), and organic matter-like (OM•) radicals. Kinetic modeling and radical quenching experiments substantiated that $SO_4^{\bullet-}$ and OM• were the main contributing species to SMX degradation. Chemical extraction, Mössbauer spectroscopy, and X-ray photoelectron spectroscopy analyses demonstrated that sediments surface-adsorbed Fe(II) predominantly interacted with PDS at a high molar Fe(II)/PDS ratio of 1.41, whereas structural Fe(II) underwent slower electron transfer reactions at a lower ratio of 0.75. This study provides novel insights into PDS activation by Fe(II)-bearing sediments and could advance the development of effective sediments-based PDS activation strategies for remediating contaminants in anoxic subsurface environments.

## 1. Introduction

The livestock farming and aquaculture industries play crucial roles in global food security, particularly in developing countries [1]. However, the extensive use of antibiotics in these industries to control infectious diseases and promote animal growth [2] has led to the accumulation of these compounds in soil [3] and groundwater [4]. As an example, sulfamethoxazole (SMX) is widely used to treat bacterial infections in humans and animals [5,6] and the continuous release of SMX into natural subsurface environments poses a potential threat to ecosystems [4,6]. Trace SMX concentrations, ranging from 1 ng/L to 5.57 mg/L, have been frequently found in samples of aquaculture water, sediment porewater, and groundwater [7]. As a consequence of such contamination, the utilization of groundwater as a drinking water resource may result in various human health issues. Thus, it is essential to remediate SMX-contaminated groundwater to prevent the spread of contaminants in subsurface environments.

Advanced oxidation processes (AOPs) have been shown to be effective in removing SMX from aqueous environments [8–10]. Radical-based AOPs using species such as hydroxyl radical (•OH) and sulfate radical ($SO_4^{\bullet-}$) have been extensively investigated and the associated SMX degradation pathways, removal efficiencies, and optimized reaction conditions have all been assessed [8]. Various laboratory-scale studies have also explored ultrasonic-catalytic oxidation [8],

* Corresponding authors.
*E-mail addresses:* liaopeng@mail.gyig.ac.cn (P. Liao), hjcui@hunau.edu.cn (H.-J. Cui).

https://doi.org/10.1016/j.cej.2023.144938
Received 11 April 2023; Received in revised form 17 July 2023; Accepted 19 July 2023
Available online 20 July 2023
1385-8947/© 2023 Elsevier B.V. All rights reserved.

photocatalysis [9], and Fenton-like methods [10] as approaches to degrading SMX in aqueous environments. However, the majority of these methods involve ectopic treatment and challenges remain related to the cost, operability, and limited understanding of the complexity of actual subsurface environments. Therefore, there is a pressing need for the development of cost-effective, simple, and environmentally-friendly *in situ* methods capable of efficiently removing SMX from anoxic subsurface environments.

In recent years, the peroxydisulfate (PDS)-based *in situ* chemical oxidation (ISCO) has emerged as a promising remediation technology for detoxifying contaminants [11–15]. Sedlak's group reported PDS-based ISCO treatments that used Fe(III) and Mn(IV) oxides to activate PDS and generate $SO_4^{\bullet-}$ and •OH over time scales of several weeks. The rates at which these radicals were generated were 2 to 20 times faster than those obtained from metal-free systems in typical groundwater [13]. Fe(II) and Fe(II)-bearing minerals, which are ubiquitous in subsurface sediments, have also been reported to activate PDS on time scales of seconds to hours as a means of remediating various contaminants [16–21]. Zhou's group established that Fe(II) in reduced nontronite NAu-2 had a significant activation effect on PDS, resulting in the degradation of diethyl phthalate within 30 s [17]. They suggested that this rapid degradation of organic contaminants was driven by surface-bound $SO_4^{\bullet-}$ and •OH in a system comprising reduced Fe-bearing smectite clays and PDS [17]. Mustapha et al. found that an Fe(II)-O complex present in sediments interacted with persulfate to produce $SO_4^{\bullet-}$, •OH, and Fe(IV) species, and that these products promoted the decomposition of aniline in groundwater [22]. These studies highlight the significant but often overlooked role of sediments in activating PDS for contaminant detoxification during ISCO treatment.

The effectiveness of ISCO depends both on the rate of PDS activation and the yield of $SO_4^{\bullet-}$ and •OH. The rates of PDS activation and oxidant yields, in turn, appear to be affected by the mineral species present in sediments and aquifers, because these minerals initiate the radical chain reactions that convert PDS into $SO_4^{\bullet-}$ and other reactive radicals [13,23,24]. Interestingly, the reactivity of Fe(II) varies significantly depending on the species in which it is found [25,26]. Recent research by our own group demonstrated the presence of various Fe(II) species in subsurface sediments, with those species exhibiting a moderate oxidation rate and •OH yield evidently being best suited to contaminant degradation [26]. Zhou's group suggested that •OH production during the oxidation of paddy soils was closely linked to the concentration of active Fe(II) species, including ion-exchangeable, surface-adsorbed, and structural Fe(II) in minimally crystalline minerals [27,28]. Therefore, the yield of radicals available for contaminant oxidation during PDS-based ISCO will be affected by the specific Fe(II) species present in the local sediments. On this basis, it is reasonably to propose that the Fe(II) species in sediments play a significant role in PDS activation to generate $SO_4^{\bullet-}$ and •OH and thus in contaminants degradation. Understanding the reaction mechanisms associated with different Fe(II) species as well as the oxidizing capacities of the various radicals produced during PDS activation by sediments is critical to the development of effective subsurface remediation strategies.

The objective of the present study was to elucidate the role of Fe(II) species in the activation of PDS by sediments during the oxidation of SMX under anoxic conditions. To this end, natural sediments collected from farmland were employed to activate PDS for SMX degradation. Throughout this process, the SMX degradation performance was examined along with the toxicity of the resulting products while activating PDS at an initial pH of 7.1. The contribution of reactive oxidizing species to SMX degradation was confirmed using electron paramagnetic resonance (EPR) spectroscopy together with radical quenching experiments and kinetic models. The stoichiometry ratio of the reaction between PDS and Fe(II) in sediments was also analyzed. In addition, chemical extraction, X-ray photoelectron spectroscopy (XPS), and Mössbauer spectroscopy were employed to investigate the dynamics of the reactions of the various Fe(II) species. Finally, the effects of operational parameters such as the amount of sediment, the PDS concentration, the initial pH and temperature, and the SMX concentration were assessed. The results of this work provide helpful insights into a new process for the activation of PDS using Fe(II)-containing sediments under anoxic conditions.

## 2. Materials and methods

### 2.1. Chemicals and sediments

The chemicals used in this work are described in the Supplementary Material (Text S1). The sediment was collected from farmland in the Jianghan Plain (113.678331° E, 104 30.175845° N) at a depth of 4.5 m in a location having a groundwater table depth of 4 m, as described in our previous study [26]. The sediment samples were tightly wrapped with foil in the field, sealed in a plastic bag under vacuum then transported to the laboratory where they were refrigerated at −20 °C in the dark until being used. The sediments contained 40.1% Fe(II) out of the total Fe(II) and a soil organic matter concentration of 9.43 g/kg. In preparation for each PDS activation experiment, the sediment was thawed and used without drying. Additionally, portions of the sediment were thawed and oxidized in air to obtain oxidized sediments.

### 2.2. SMX degradation with PDS activation by sediments

The degradation of SMX using PDS combined with the sediments was carried out in 100 mL bottles under anoxic conditions. In a typical trial, three bottles were each filled with 50 mL of a suspension containing 10 g/L sediment (equivalent to an Fe(II) concentration of 1.4 mM), 10 μM SMX, and 2.2 mM PDS, working in an anaerobic glove chamber (Mikrouna Co., Ltd., China). These bottles were subsequently wrapped with aluminum foil to exclude light during the reaction process and each suspension was then stirred with a Teflon-coated magnetic stir bar at 300 rpm for 60 min. For most case, the initial pH suspension was 7.1 and the pH was not adjusted throughout the experiments. However, because of the decomposition of PDS to produce $SO_4^{2-}$ and $H^+$ ions via the reaction $S_2O_8^{2-} + H_2O \rightarrow 2SO_4^{2-} + 2H^+ + 1/2O_2$ [29], the pH was found to decrease to 3.5 by the end of the 60 min reaction (Fig. S1). The effects of various parameters on SMX degradation were studied, including the sediment concentration (using 5, 10, and 20 g/L), PDS concentration (1, 1.5, and 2.2 mM), initial pH (5, 6, 7.1, and 8), temperature (18, 25, and 34 °C) and SMX concentration (2.5, 5, 10, and 15 μM). Control experiments of SMX degradation by PDS, sediments, and PDS/oxidized-sediments were also performed. Throughout the 60 min reaction, an approximately 3 mL aliquot of each suspension was withdrawn at regular intervals and immediately passed through a 0.22 μm filter under vacuum. The solid particles that were captured were analyzed for Fe(II) content while the concentrations of dissolved $Fe^{2+}$ ions, SMX, PDS, and TOC in the filtrate were also determined. To further assess the degradation efficiency of this system, trials using tetracycline (TC, 10 μM) and ciprofloxacin (CIP, 10 μM) were also performed. All experiments were performed at least in triplicate.

### 2.3. Relative contributions of minerals and organic matter

The relative contributions of minerals and organic matter in the sediment to the activation of PDS for SMX degradation were determined by extracting the organic matter from the sediment prior to some trials. Working in an anoxic glove box, the organic matter was extracted from a 0.5 g portion of sediment using 50 mL of a NaOH solution having a pH of 12 over a time span of 12 h. This extraction was repeated three times after which the extracts were filtered under vacuum [30,31]. This procedure was found to remove approximately 70% of the soil organic matter in the sediment. Following this procedure, the remaining solid was mixed with 50 mL of deionized water. The pH values of both the filtrate and the solid suspension were adjusted to 7.1 before the addition

of SMX and PDS in subsequent trials.

### 2.4. Analyses and characterization

The concentrations of SMX, CIP, and TC in the various samples were measured by using high performance liquid chromatography (HPLC) (LC-20A, Shimadzu, Japan), as described in Text S2. The identities of the intermediate products generated during degradation of the SMX were established using a Quadrupole Time of Flight mass spectrometer (Agilent Q-TOF 6550) coupled with an Ultra Performance Liquid Chromatography system (Agilent 1290 UPLC) (UPLC-Q-TOF-MS), as described in Text S3. Changes in the total organic carbon (TOC) value of the aqueous phase after SMX degradation were monitored with a TOC analyzer (Shimadzu TOC-LCPH, Japan). The toxicities of the SMX degradation products were evaluated by assessing the degree to which the luminescence of *Photobacterium phoshoreum T3 spp* was affected, based on the method provided in Text S4.

The concentration of PDS was determined by adding a solution containing 3 M KI and 0.29 M $NaHCO_3$ to each sample followed by centrifugation, after which the supernatant absorbance at 400 nm was obtained using a UV–vis spectrophotometer (UVmini-1280, Shimadzu, Japan) [20]. Total Fe(II) concentrations were determined by adding 1 mL of each suspension sample to 9 mL of a solution containing 1.3 M HF, 5 M HCl and 1.8 M $H_2SO_4$ and heating the mixture at 80 °C for 1 h. The Fe(II) level was subsequently ascertained based on the absorbance at 510 nm using the 1,10-phenanthroline method, with a detection limit of 0.02 mg/L [32,33]. The presence of $F^-$ can shield Fe(III), and so the interference of Fe(III) with the Fe(II) analysis was considered negligible [34]. Total Fe was measured after reducing Fe(III) in each acidified sample by adding 10% hydroxylamine hydrochloride.

Sequential extractions of both the as-received and oxidized sediment samples were performed to identify the various Fe(II) species present under anoxic conditions, including dissolved $Fe^{2+}$, ion exchangeable Fe (II), adsorbed Fe(II), and structural Fe(II). During the activation of PDS by the sediment, different Fe(II) species were extracted at pre-determined time intervals. Dissolved $Fe^{2+}$ was obtained by taking a 2 mL aliquot of the suspension and passing this sample through a filter under vacuum, after which the level of dissolved $Fe^{2+}$ in the filtrate was ascertained. Ion exchangeable Fe(II) was measured by extracting each solid sample with 10 mL of a 1 M $CaCl_2$ solution (pH 7.0) for 4 h [27,35]. The resulting suspension was filtered and the filtrate was then analyzed for Fe(II). To determine surface-adsorbed Fe(II), the remaining solids were extracted with 10 mL of a 1 M solution of $NaH_2PO_4$ (pH 5.0) under anoxic conditions for 18 h [26,36]. After filtration, the amount of surface-adsorbed Fe(II) in the filtrate was found. The residual structural Fe(II) in the solid was obtained by extraction with 10 mL of a solution containing 1.3 M HF and 1.8 M $H_2SO_4$ at 80 °C for 1 h [37]. All the sequential extractions were performed at least in triplicate.

EPR spectroscopy was used to identify the free radicals formed in the sediments during activation of the PDS. XPS spectra were acquired to ascertain the various Fe redox states in the sediment throughout the reaction. Mössbauer spectra of the sediments were also obtained at 13 K to examine variations in Fe coordination during the reaction. These characterizations are described in detail in Text S5.

## 3. Results and discussion

### 3.1. PDS activation by sediments for SMX degradation

Fig. 1a demonstrates that SMX concentration decreases slightly (<5.6%) after 60 min in the presence of oxidized sediment (Fe(III)/$Fe_{total}$ = 100%) and PDS or PDS alone. Under these conditions, PDS decomposed slightly as well (Fig. 1b). These results indicate that Fe(III)-based minerals in the oxidized sediments had only a very limited capability to activate PDS for SMX degradation during the time span examined in this study. In contrast, in the presence of the sediments (Fe

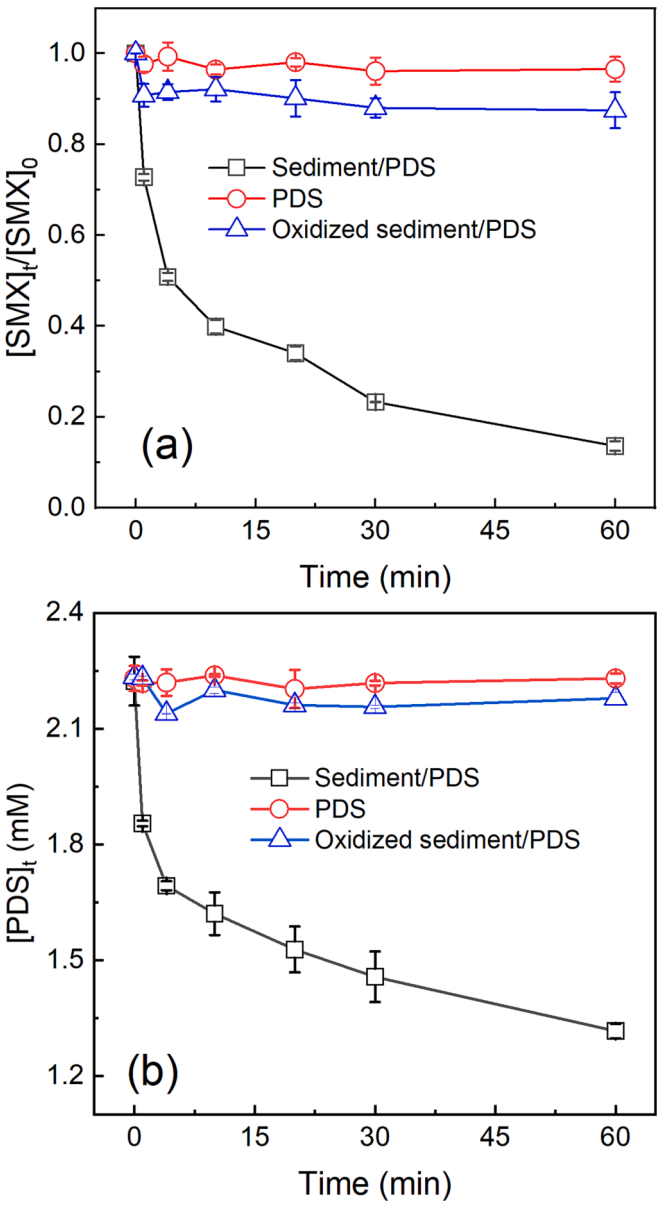


**Fig. 1.** (a) SMX degradation and (b) PDS decomposition as functions of time during trials with PDS activated by sediment. Reaction conditions: $[PDS]_0$ = 2.2 mM; $[SMX]_0$ = 10 μM; sediment (40.1% Fe(II) in total Fe) = 10 g/L; and 25 ± 1 °C.

(II)/$Fe_{total}$ = 40.1%) and PDS, the concentration of SMX rapidly decreased from 10 to 4 μM within 10 min and then gradually declined to 1.34 μM within 60 min under anoxic conditions (Fig. 1a). The corresponding decrease in the TOC after 60 min was approximately 0.41 mg/L (Text S6, Table S1), equivalent to a 33.6% drop. Concurrently, the PDS concentration decreased from 2.2 to 1.31 mM over the same duration (Fig. 1b) and the SMX degradation exhibited a linear correlation with the extent of PDS decomposition (Fig. S2). The slope of this plot corresponded to the extent of SMX degradation (1 μM) associated with the decomposition of one unit of PDS concentration (1 mM). In this manner, the PDS utilization efficiency for SMX degradation was determined to be approximately 1.0% in the sediment/PDS system. These results suggest that reduced species, including soil organic matter (SOM) and Fe(II)-bearing minerals in the sediment, were likely the primary factors activating the PDS for SMX degradation. However, only approximately 4.5% of the SMX was degraded when the PDS was activated solely by the extracted organic matter (Fig. S3). Hence, Fe(II) and its mineral phases

might be the main factors involved in the activation of PDS.

As noted, the degradations of two other typical antibiotics (TC and CIP) were examined and Fig. S4 demonstrates that amounts greater than 78% of both antibiotics were removed from the reaction system within 60 min. These high degradation efficiencies confirm the effectiveness of the sediment/PDS system as a means of degrading antibiotics in PDS-based ISCO treatments.

### 3.2. Identification of the reactive oxidizing species for SMX degradation

EPR analyses were conducted to investigate the production of reactive oxidizing species during trials in which PDS was activated by sediment under anoxic conditions. No signal was generated by the oxidized sediment/PDS system under anoxic conditions, indicating negligible concentrations of free radicals (Fig. 2). In contrast, the sediment/PDS system in which the sediment contained Fe(II) provided a strong EPR signal comprising four lines with an intensity ratio of 1:2:2:1 ($a_N = a_H = 14.8$ G). These data are consistent with the signal expected from DMPO-OH (Fig. 2a). A six-line signal with a ratio intensity of 1:1:1:1:1:1 also accompanied the formation of DMPO-OH, possibly attributable to DMPO-$SO_4$ ($a_N = 13.9$, $a_H = 10.2$ G) [11,38]. A second six-line signal with the same 1:1:1:1:1:1 intensity ratio was also identified, likely originating from the reaction of OM• with DMPO [39]. It has been reported that •OH is rapidly quenched by SOM to generate OM• [39,40]. Moreover, a triplet EPR peak associated with singlet oxygen ($^1O_2$) was not observed [41], indicating the absence of $^1O_2$ in the sediment/PDS system (Fig. S5). Therefore, •OH, $SO_4^{\bullet-}$, and OM• radicals were produced during the trials in which the sediment activated PDS under anoxic conditions (Fig. 2).

To assess the contribution of OM• to the SMX degradation process, a portion of SOM was initially removed from the sediment by extraction. Following this removal of SOM, 72.7% of the SMX was degraded, representing a decrease in efficiency compared with the earlier value of 86.4%. This observation indicated that OM• generated from the SOM were involved in the SMX degradation mechanism. The contribution of •OH was also assessed by performing trials in which *tert*-butanol (TBA) was added, based on the reaction rate constants $k_1$ (TBA, $SO_4^{\bullet-}$) = $2.3 \times 10^5$ $M^{-1}$ $s^{-1}$ and $k_2$ (TBA, •OH) = $6 \times 10^8$ $M^{-1}$ $s^{-1}$ [42,43]. The rate constant for the reaction of SMX with •OH is approximately an order of magnitude greater at $7.9 \times 10^9$ $M^{-1}$ $s^{-1}$ [44], indicating that nearly all the •OH (>98%) should be consumed by TBA in the case that the TBA concentration (10 mM) is 1000 times higher than that of the SMX. However, the presence of 10 mM TBA barely inhibited SMX degradation (such that 85% of the SMX was degraded), confirming that •OH was not involved in SMX degradation to any appreciable extent in the sediment/PDS system under anoxic conditions. The contribution of $SO_4^{\bullet-}$ to SMX degradation was examined by adding ethanol ($k_3$ (ethanol, •OH) = $1.2–2.8 \times 10^9$ $M^{-1}$ $s^{-1}$, $k_4$ (ethanol, $SO_4^{\bullet-}$) = $1.6–7.7 \times 10^7$ $M^{-1}$ $s^{-1}$, and $k_5$ (SMX, $SO_4^{\bullet-}$) = $1.2 \times 10^{10}$ $M^{-1}$ $s^{-1}$) to the reaction system. The value of *ck* (*c* is the concentration of the probes, and *k* is the reaction rate constant of the probes with $SO_4^{\bullet-}$) is used to compare the competitive capacity of the probes for $SO_4^{\bullet-}$. Because the *ck* of 100 mM ethanol for $SO_4^{\bullet-}$ is 13–64 times greater than that of 10 μM SMX [43,45–47], 100 mM ethanol would be expected to react with nearly all the $SO_4^{\bullet-}$ produced. Results show that the degradation efficiency of SMX was significantly inhibited following the addition of 100 mM ethanol, decreasing from 86.4% to 20.0%. Moreover, a further inhibition was observed with the addition of 2.5 M ethanol (Fig. 2b). These results suggest that $SO_4^{\bullet-}$ radicals were mainly involved in SMX degradation. Further, quantitative estimations based on a process-based kinetic modeling established that the relative contributions of $SO_4^{\bullet-}$, OM•, and •OH to this process were 65.4%, 21.2%, and nil, respectively (Text S7, Fig. S6 and Table S2). Evidently, $SO_4^{\bullet-}$ and OM• radicals were entirely responsible for the SMX degradation, with the former likely playing a major role.

### 3.3. Identification of Fe(II) species in sediment involved in PDS activation

The oxidation of Fe(II) was also monitored as a means of gaining additional insights into the reaction mechanism. In trials combining sediment and PDS, Fe(II) was oxidized rapidly (within the initial 1 min) and the reaction proceeded at a slower rate (Fig. 3a and b). Specifically, the Fe(II) concentration was reduced by 0.52 mM over the first 1 min while only 0.38 mM was lost from that point up to 60 min. The data also indicated that dissolved $Fe^{2+}$ ions (representing < 0.1% of the total Fe (II) in the sediment) and total dissolved Fe (less than < 0.1% of the total Fe in the sediment) in the solution could be negligible during the reaction between the sediment and PDS (Fig. S7). Our previous work demonstrated that sediments contain ion-exchangeable, surface-adsorbed Fe(II) together with structural Fe(II) in minerals [26]. To further understand the role of these Fe(II) species in PDS activation, sequential extractions were conducted to analyze the exchangeable Fe(II) (referred to herein as $CaCl_2$-Fe(II)), surface-adsorbed Fe(II) ($NaH_2PO_4$-Fe(II)) and mineral structural Fe(II) (HF-$H_2SO_4$-Fe(II)) (Fig. 3b). The sediment was found to contain 0.07 mM exchangeable Fe(II), 0.59 mM surface-adsorbed Fe(II), and 0.77 mM mineral structural Fe(II). In addition, the exchangeable Fe(II) was almost completely oxidized within 1 min upon mixing with the PDS. The surface-adsorbed Fe(II) concentration was also dramatically decreased (to 0.14 mM) after 1 min, with further decreases to 0.08 mM at 4 min and to 0.02 mM at 60 min. The mineral structural Fe(II) was oxidized slowly throughout the entire reaction time, with a decrease of 0.27 mM over 60 min. Therefore, the abundant surface-adsorbed Fe(II) appears to actively participate in PDS

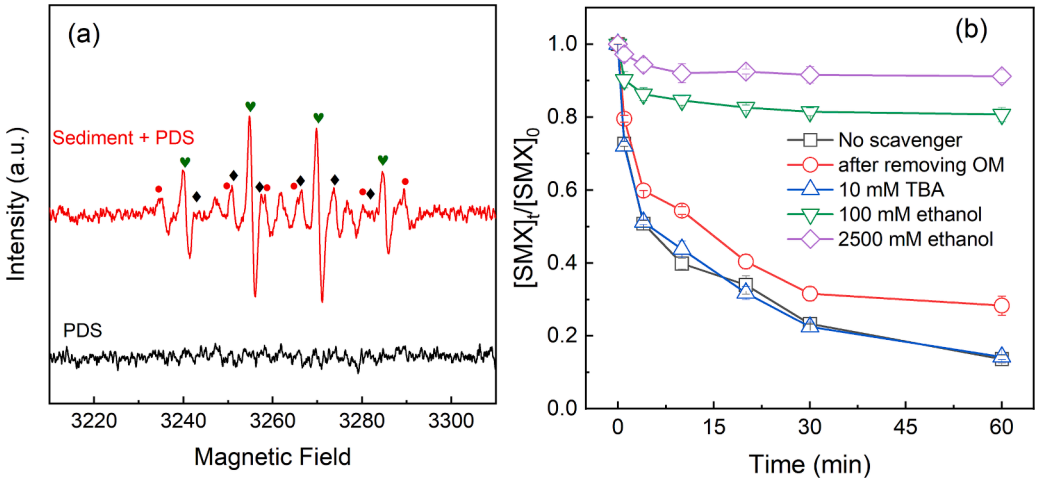


**Fig. 2.** (a) EPR spectra indicating the presence of free radicals in sediment/PDS systems. Legend: green hearts: DMPO-OH, black diamonds: DMPO-$SO_4$, red circles: DMPO-OM. (b) SMX degradation after removing OM and in the presence of radical scavengers (TBA and ethanol). Reaction conditions: $[PDS]_0$ = 2.2 mM; $[SMX]_0$ = 10 μM; sediment (40.1% Fe(II) in total Fe) = 10 g/L and 25 ± 1 °C. (For interpretation of the references to colour in this figure legend, the reader is referred to the web version of this article.)

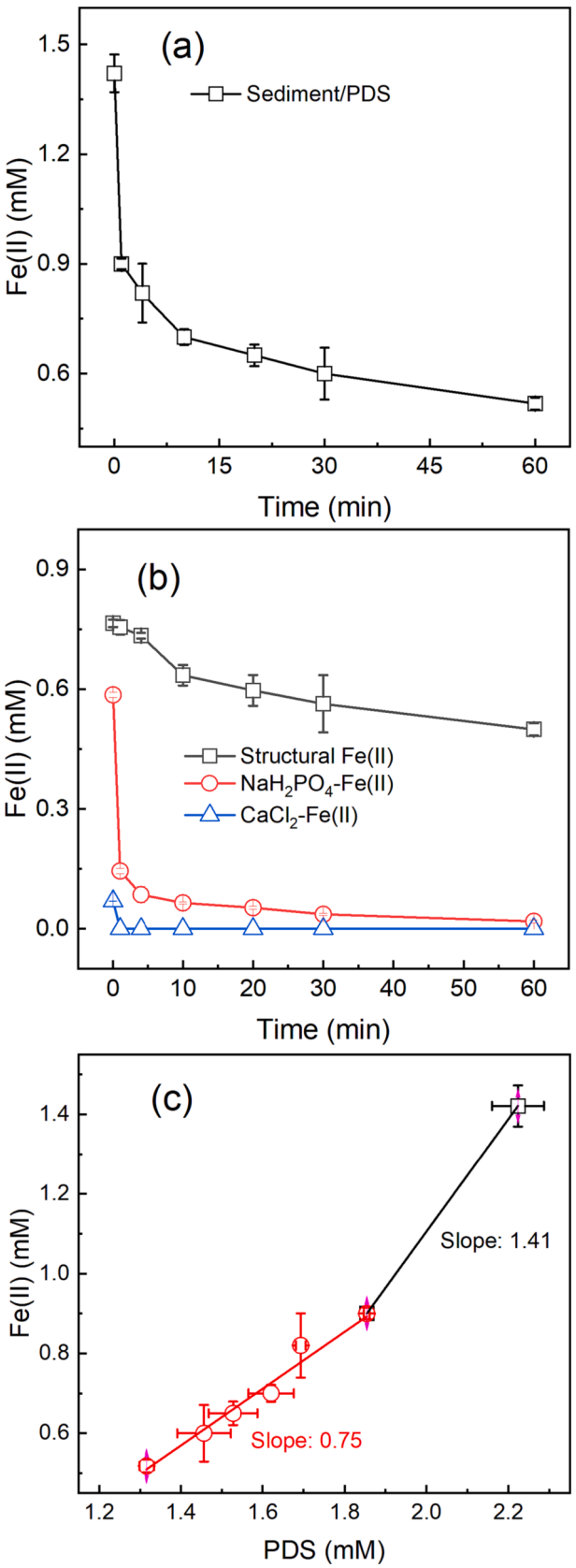


**Fig. 3.** Variation of (a) total Fe(II) and (b) Fe(II) species, and (c) correlation between PDS and Fe(II) in sediment/PDS system. Reaction conditions: $[PDS]_0$ = 2.2 mM; $[SMX]_0$ = 10 μM; sediment (40.1% Fe(II) in total Fe) = 10 g/L; 25 ± 1 °C.

decomposition during the initial 1 min while the structural Fe(II) decomposes the PDS more slowly.

An assessment of the relationship between PDS decomposition and Fe(II) oxidation indicated a two-stage correlation (Fig. 3c). The slope of this linear plot was 1.41 during the initial 1 min but decreased to 0.75 after that point. This slope represents the change in the Fe(II) concentration (in mM) resulting from oxidation ratio to the decomposition of a unit PDS concentration (that is, 1 mM). Previous studies have reported a theoretical stoichiometric ratio of 2:1 between changes in the $Fe^{2+}$ and PDS concentrations [45,48], which is much higher than the values obtained from the present work. Additionally, control experiments showed that the Fe(II) oxidation amount (ΔFe(II)) increased from 0.95 to 1.20 mM after 60 min during the mineral phase activating PDS, whereas the PDS decomposition decreased from 0.91 to 0.71 mM. These results suggest that the stoichiometric ratio between Fe(II) and PDS in this reaction increased to 1.69 (Table S3). The decrease in the PDS concentration by SOM extracted from the sediment was small (0.05 mM), indicating that the SOM did not directly react with the PDS. However, the SOM may have indirectly affected the reaction by changing the stoichiometric ratio between Fe(II) and PDS. Because PDS is a strong oxidant, the high concentration of reactive Fe(II) in the sediment greatly promoted PDS decomposition, leading to a higher stoichiometric ratio of Fe(II) to PDS in the initial stage of the reaction. In the later stage, because the structural Fe(II) was less active, the OM preferentially reacts with •OH via H-abstraction processes to generate OM•. The latter activated the PDS to produce $SO_4^{\bullet-}$ via electron transfer [39,49,50]. This process may have been partly responsible for the low stoichiometric ratio of Fe(II) to PDS.

To further explore the changes in Fe(II) speciation during the reaction, 13 K Mössbauer spectra were acquired from the sediment specimens (Fig. 4, Table S4). The fitted spectra showed two Fe(II) signals, related to Fe(II)-silicates and surface-adsorbed Fe(II). Following the reaction, the surface-adsorbed Fe(II) rapidly decreased, from 7.0% to nil, within 1 min, while the Fe(II)-silicates only decreased by 1.6%. In addition, the proportion of Fe(III) oxides increased from 30.0% to 44.7%. These changes suggested that surface-adsorbed Fe(II) was preferentially oxidized to produce Fe(III) oxides during the reaction. Following a 60 min reaction, the proportion of Fe(II)-silicates gradually decreased from 27.8% to 18.2% while the proportions of Fe(III)-silicates and Fe(III) oxides increased from 27.5% to 32.9% and from 44.7% to 48.9%, respectively. It is therefore apparent that a portion of the Fe(II)-silicates was directly oxidized to generate Fe(III)-silicates while another portion was oxidized to Fe(III) oxides by the PDS. Interestingly, there was also a decrease of 6.6% in the Fe(III)-silicates after the initial 1 min, possibly related to a transformation into Fe(III) oxides. The extent of Fe leakage into the solution was negligible (Fig. S7), suggesting that the transfer of near surface structural Fe(III) and Fe(II) in silicates to the mineral surfaces may have occurred as the pH of the suspension decreased during the reaction. The newly formed Fe(III) oxides resulting from these processes might have participated in PDS activation [39].

To further explore variations in the near-surface Fe(II) during the activation of PDS, Fe $2p_{3/2}$ XPS data were collected [17,51]. As shown in Fig. 5, the Fe(II) content was dramatically decreased, from 32.2% to 22.4%, after 1 min of reaction. However, past this point and up to 60 min, the surface Fe(II) proportion as determined by XPS remained almost constant at approximately 22.1% (Table S5). These XPS observations indicated higher Fe(II) concentrations compared with the values obtained by acidic dissolution, and so it is possible that a greater amount of Fe(II) was distributed near the surface after 1 min of the reaction. Based on the relatively constant near-surface Fe(II) concentration over the time span of 1 to 60 min during the oxidation process, it appears that surface Fe(II) oxidized by PDS could be regenerated by electrons transferred from the bulk structural Fe(II). This hypothesis is consistent with a recent study showing the regeneration of reactive surface Fe(II) during sediment oxidation [26]. In summary, both the XPS and Mössbauer spectra demonstrated that surface-associated Fe(II) was

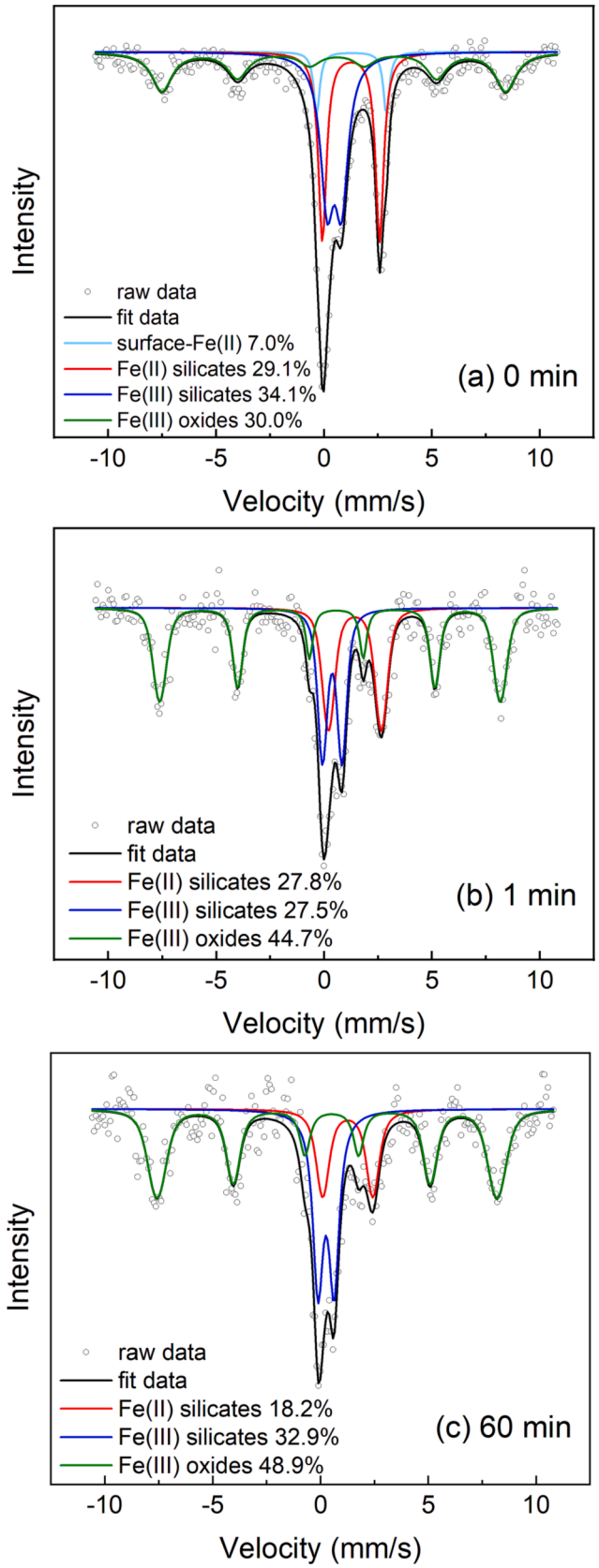


**Fig. 4.** Mössbauer spectra of sediments at different stages of persulfate activation. The fitted Mössbauer parameters are summarized in Table S4. Reaction conditions: $[PDS]_0$ = 2.2 mM; $[SMX]_0$ = 10 μM; sediment (40.1% Fe(II) in total Fe) = 10 g/L; 25 ± 1 °C.

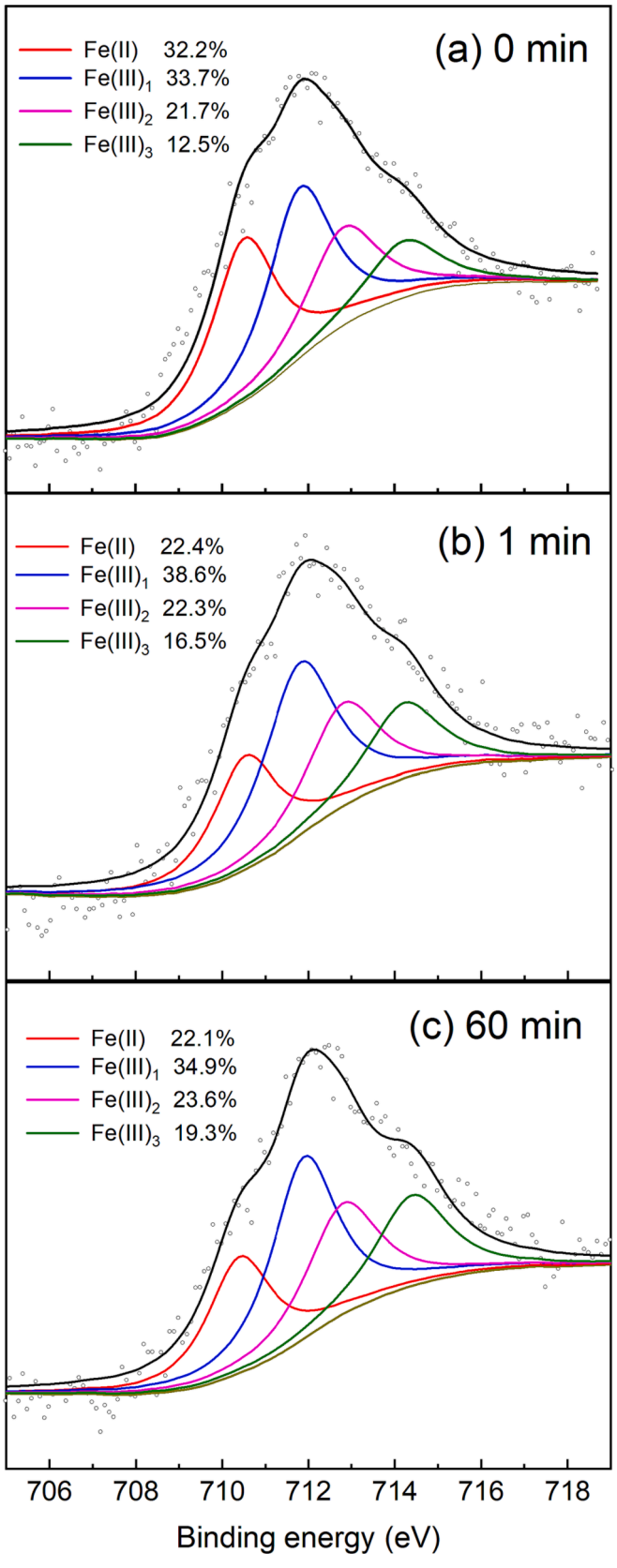


**Fig. 5.** XPS spectra acquired from sediment at different stages of PDS activation. The Fe 2p3/2 peaks were assigned based on literature-reported values [17,51]. Reaction conditions: $[PDS]_0$ = 2.2 mM; $[SMX]_0$ = 10 μM; sediment (40.1% Fe(II) in total Fe) = 10 g/L; 25 ± 1 °C.

preferentially oxidized while structural Fe(II) was oxidized slowly through electron transfer.

### 3.4. Mechanisms of PDS activation by sediments for SMX degradation and toxicity removal under anoxic conditions

Based on the above results, the reaction pathways for PDS activation by sediments in conjunction with SMX degradation under anoxic conditions can be proposed (Fig. 6). In these processes, the Fe(II) in the mineral phases of the sediment plays a primary and direct role in PDS activation. In the initial stage, surface-adsorbed Fe(II) preferentially and rapidly interacts with the PDS to generate $SO_4^{\bullet-}$ and Fe(III) oxides at a high stoichiometric ratio of Fe(II) to PDS. The $SO_4^{\bullet-}$ resulting from this process can partially oxidize –OH from water dissociation or mineral-bound hydroxyl groups to produce •OH. These •OH and $SO_4^{\bullet-}$ radicals react with SOM via H-abstraction processes to form OM•. Subsequently, structural Fe(II) reacts slowly with PDS via an electron transfer process. Additionally, OM• radicals participate in PDS activation, producing $SO_4^{\bullet-}$ through electron transfer [50] and lowering the stoichiometric ratio of Fe(II) to PDS. Consequently, although the contribution of SOM to PDS decomposition can be negligible, the intermediate OM• radicals serve to promote the formation of $SO_4^{\bullet-}$ from the PDS. Among the various reactive species ($SO_4^{\bullet-}$, •OH, and OM•), the $SO_4^{\bullet-}$ is the primary driver of SMX degradation while OM• has a minor role based on promoting the formation of $SO_4^{\bullet-}$. In contrast, •OH has limited involvement in SMX degradation.

During the reactions, the products TP 174, TP 114, TP 268 and TP 284 were identified by UPLC-Q-TOF-MS/MS and two possible SMX oxidation mechanisms were devised (Fig. 6 and S8). Previous studies have demonstrated that SMX can undergo chemical and biological hydrolysis along with the formation of 4-amino benzene sulphinic acid and 3-amino-5-methylisoxazole [16,52]. The TP 174 and TP 114 identified in the present work could represent the former and latter compounds, resulting from oxidation of the methyl group on 3-amino-5-methylisoxazole to produce the aldehyde group on TP 114 (pathway 1, Fig. 6). In pathway 2, the appearance of nitroso-SMX (TP 268) could result from the oxidation of the $–NH_2$ group of SMX by OM• and $SO_4^{\bullet-}$ radicals with the subsequent transition of this compound to nitro-SMX (TP 284) [40,52].

Following the degradation of 10 μM SMX in a sediment/PDS system for 60 min, the toxicity of the sample towards *Photobacterium phoshoreum T3 spp* decreased, from 46% to 27%. However, it is important to note that some of the intermediate products appeared to exhibit some toxicity towards *Photobacterium phosphoreum T3 spp*, as evidenced by the inhibition of the sample luminescence at 60 min (with 1.36 μM SMX remaining) being higher than that observed with 2 μM SMX (Table S6, Text S4). It has been reported that aniline can damage bacterial DNA and so can be toxic to these microorganisms [53]. Thus, it is likely that the aniline moieties in TP 174 and TP 114 were harmful to the *Photobacterium phosphoreum T3 spp* (pathway 1), while oxidation of the $–NH_2$ group of SMX (pathway 2) and mineralization of SMX (Table S1) might be responsible for the decreased SMX toxicity.

### 3.5. Effects of the operating parameters on SMX degradation

In additional trials, the sediment amount, PDS concentration, initial pH, temperature and SMX concentration were all varied. Fig. 7a demonstrates that the extent of SMX degradation after 60 min increased from 65.8% to 86.4% with an increase in the PDS concentration from 1.0 to 2.2 mM. Correspondingly, Fe(II) oxidation and PDS decomposition concentrations were increased by 0.22 and 0.28 mM, respectively (Table S7). Hence, the PDS concentration was a key factor affecting the degree of SMX degradation. Fig. 7b shows that increasing the sediment concentration from 5 to 20 g/L had little effect on the SMX degradation efficiency (with an increase from 80.9% to 89.5%) but did drastically enhance Fe(II) oxidation and PDS decomposition (Table S8). Increasing the amount of sediment would also increase the SOM concentration in the system and this material would compete with the SMX for the •OH or $SO_4^{\bullet-}$, leading to a slight improvement in SMX degradation. This competitive process was confirmed by the TOC data and by the observation of OM• formation in the sediment/PDS system (Table S1). The OM• radicals formed as intermediates would additionally be expected to promote PDS decomposition [39] and this effect could increase the costs associated with ISCO treatments based on PDS.

Upon increasing the temperature from 15 to 34 °C in the sediment/PDS system, the extent of degradation of 10 μM SMX was increased from 76.7% to 94%% after 60 min (Fig. 7c). Simultaneously, the PDS decomposition was increased from 0.79 to 1.11 mM (Table S9). Previous studies have reported the formation of $SO_4^{\bullet-}$ as a consequence of the thermal activation of PDS [54,55], suggesting that the *in situ* degradation of SMX by sediment/PDS is promoted at higher temperatures.

Fig. 7d provides data showing that the extent of SMX decomposition was closely correlated with the initial pH over the range of 5.0–8.0. Specifically, the SMX degradation after 60 min decreased from 99.5% to 86.4% as the pH was increased from 5.0 to 7.1. However, SMX degradation at the 60 min was significantly inhibited when the pH was increased to 8.0 (giving an efficiency of 28.7%). This change was attributed to decreased PDS decomposition (Table S10) resulting from electrostatic repulsion between PDS anions and the sediment surface [17,56]. These results indicate that the sediment/PDS system was capable of the highly efficient decomposition of SMX at initial pH values below 7.1.

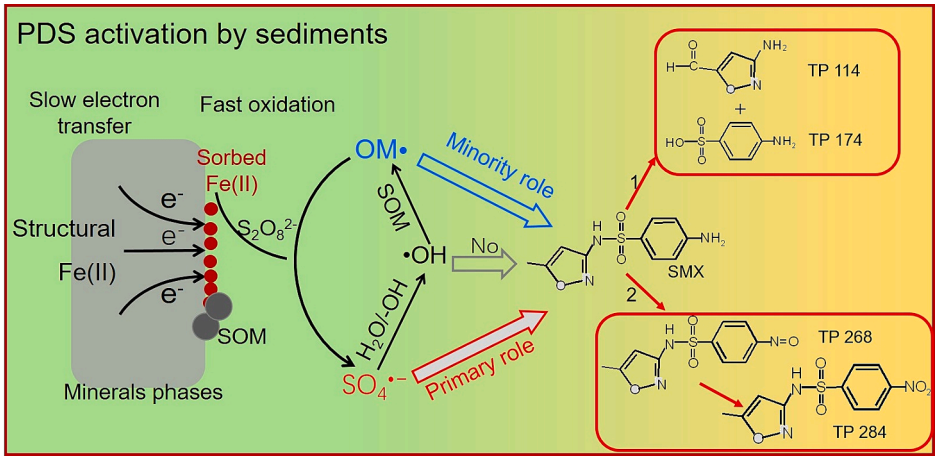


**Fig. 6.** Proposed mechanisms for PDS activation by sediments for SMX degradation under anoxic conditions.

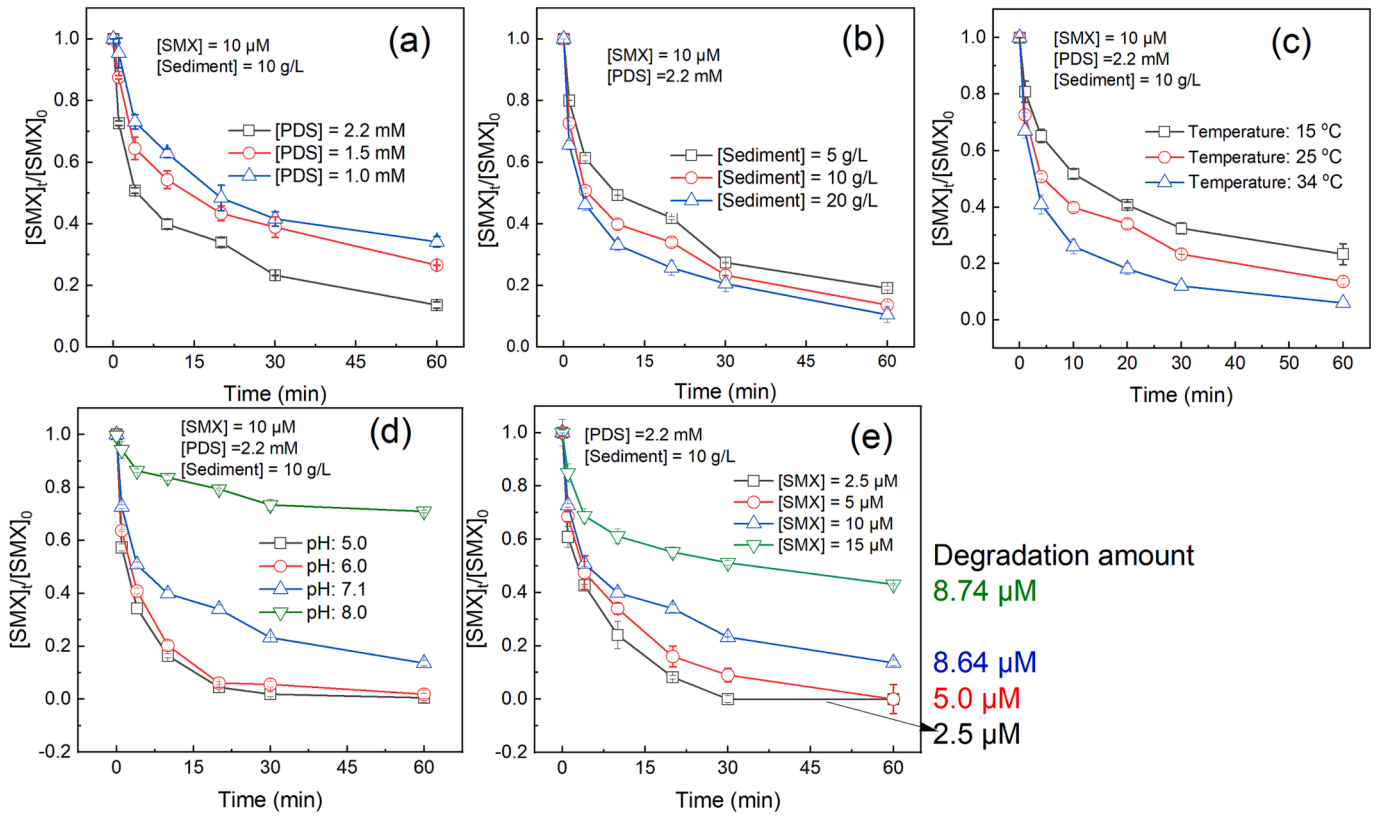


**Fig. 7.** Effects of (a) the PDS concentration, (b) the amount of sediment, (c) the temperature, (d) the pH, and (e) the SMX concentration on SMX degradation.

The effect of the SMX concentration was also investigated (Fig. 7e). When the initial SMX concentration was increased from 2.5 to 10 μM, the SMX degradation was decreased from 100% to 86.4%. However, upon increasing the initial SMX concentration from 10 to 15 μM, the degradation efficiency was decreased to 57.0% to give a value of 8.74 μM that was almost equivalent to a decrease of 10 μM. This finding suggested that the reaction sites might have become saturated at an initial SMX concentration of 10 μM. The sediment/PDS system demonstrated herein is therefore expected to be applicable to the degradation of SMX at low concentrations.

## 4. Conclusions

In this study, we present the first investigation of an *in situ* process involving sediment-based PDS activation for the degradation of typical antibiotics under environmentally relevant anoxic conditions. Results demonstrate that solid Fe(II) in sediments are able to greatly promote the ability of PDS to degrade antibiotics under anoxic conditions. Toxicity assessments confirmed a decrease in the toxicity of samples towards *Photobacterium phoshoreum T3 spp* after SMX degradation in sediment/PDS systems. On this basis, the sediment-based PDS process demonstrated herein appears to be an efficient and environmentally-friendly approach to the remediation of typical antibiotics. This work also elucidates previously undiscovered free radical mechanisms associated with SMX degradation in sediment/PDS systems. $SO_4^{\bullet-}$ was identified as the primary reactive oxidizing species responsible for SMX degradation, with a lesser contribution from OM•. In contrast, the effect of •OH on SMX degradation can be negligible. Surface-adsorbed Fe(II) in the sediments was found to preferentially and quickly interact with the PDS whereas structural Fe(II) reacted more slowly based on electron transfer. The transformation of Fe(II) and Fe(III) silicates to Fe(III) oxides was observed and this process affected the degree of PDS activation and thus the extent of antibiotic degradation. Further research is needed to quantify the role of mineral transformation in the interplay between PDS activation and antibiotic removal to further enhance the efficiency of this process. Considering the abundance of Fe(II) and Fe(II)-based minerals in subsurface anoxic environments, PDS activation by Fe(II)-containing sediments is expected to play a crucial role in the remediation of antibiotics by reactive oxidizing species generated *in situ* under natural anoxic conditions.

## Declaration of Competing Interest

The authors declare that they have no known competing financial interests or personal relationships that could have appeared to influence the work reported in this paper.

## Data availability

Data will be made available on request.

## Acknowledgments

This work was financially supported by the Natural Science Foundation of China (Nos. 42277291, 42107086, 41771272), Natural Science Foundation of Hunan Province (2021JJ40256), State Key Laboratory of Biogeology and Environmental Geology, China University of Geosciences (GBL22109), Thousand Innovation and Entrepreneurship Talents of Guizhou Province (NO GZQ202208091), Open Foundation of Hebei Key Laboratory of Wetland Ecology and Conservation (hklk202302), and Opening Fund of the State Key Laboratory of Environmental Geochemistry (SKLEG2023202).

## Appendix A. Supplementary data

Supplementary data to this article can be found online at https://doi.org/10.1016/j.cej.2023.144938.

## References


[1] M. Reverter, S. Sarter, D. Caruso, J.C. Avarre, M. Combe, E. Pepey, L. Pouyaud, S. Vega-Heredia, H. de Verdal, R.E. Gozlan, Aquaculture at the crossroads of global warming and antimicrobial resistance, Nat. Commun. 11 (2020) 1.

[2] Y.T. Shao, Y.P. Wang, Y.W. Yuan, Y.J. Xie, A systematic review on antibiotics misuse in livestock and aquaculture and regulation implications in China, Sci. Total Environ. 798 (2021), 149205.

[3] X.J. Tang, C.L. Lou, S.X. Wang, Y.H. Lu, M. Liu, M.Z. Hashmi, X.Q. Liang, Z.P. Li, Y. L. Liao, W.J. Qin, F. Fan, J.M. Xu, P.C. Brookes, Effects of long-term manure applications on the occurrence of antibiotics and antibiotic resistance genes (ARGs) in paddy soils: Evidence from four field experiments in south of China, Soil Biol. Biochem. 90 (2015) 179–187.

[4] S.M. Zainab, M. Junaid, N. Xu, R.N. Malik, Antibiotics and antibiotic resistant genes (ARGs) in groundwater: A global review on dissemination, sources, interactions, environmental and human health risks, Water Res. 187 (2020), 116455.

[5] G. Prasannamedha, P.S. Kumar, A review on contamination and removal of sulfamethoxazole from aqueous solution using cleaner techniques: Present and future perspective, J. Clean Prod. 250 (2020), 119553.

[6] M. Carrillo, G.C. Braun, C. Siebe, W. Amelung, J. Siemens, Desorption of sulfamethoxazole and ciprofloxacin from long-term wastewater-irrigated soils of the Mezquital Valley as affected by water quality, J. Soil Sediment. 16 (2016) 966–975.

[7] M. Zhao, X.H. Ma, X.R. Liao, S.Y. Cheng, Q. Liu, H.F. Wang, H. Zheng, X.Y. Li, X. X. Luo, J. Zhao, F.M. Li, B.S. Xing, Characteristics of algae-derived biochars and their soemediation performance for sulfamethoxazole in marine environment, Chem. Eng. J. 430 (2022), 133092.

[8] R. Zhang, Y. Yang, C.-H. Huang, N.a. Li, H. Liu, L. Zhao, P. Sun, UV/$H_2O_2$ and UV/PDS treatment of trimethoprim and sulfamethoxazole in synthetic human urine: transformation products and toxicity, Environ. Sci. Technol. 50 (5) (2016) 2573–2583.

[9] Z.Y. Dong, L. Zhang, J. Gong, Q. Zhao, Covalent organic framework nanorods bearing single Cu sites for efficient photocatalysis, Chem. Eng. J. 403 (2021), 126383.

[10] H.-J. Cui, Y.Q. Ning, C. Wu, W. Peng, D. Cheng, L.C. Yin, W.J. Zhou, W.J. Liao, Role of interfacial electron transfer reactions on sulfamethoxazole degradation by reduced nontronite activating $H_2O_2$, J. Environ. Sci. 123 (2022) 688–698.

[11] W.T Zheng, S.J. You, Y. Yao, N. R., B. D., F. L., Y.B. Liu. Sustainable Generation of Sulfate Radicals and Decontamination of Micropollutants via Sequential Electrochemistry. Engineering, (2023) doi.org/10.1016/j.eng.2022.12.005.

[12] W.T. Zheng, Y.B. Liu, F.Q. Liu, Y. Wang, N.Q. Ren, S.J. You, Atomic hydrogen in electrocatalytic systems: generation, identification, and environmental applications, Water Res. 223 (2022), 118994.

[13] H.Z. Liu, T.A. Bruton, F.M. Doyle, D.L. Sedlak, In Situ chemical oxidation of contaminated groundwater by persulfate: decomposition by Fe(III)- and Mn(IV)-containing oxides and aquifer materials, Environ. Sci. Technol. 48 (2014) 10330–10336.

[14] W.-D. Oh, Z.L. Dong, T.-T. Lim, Generation of sulfate radical through heterogeneous catalysis for organic contaminants removal: Current development, challenges and prospects, Appl. Catal. B Environ. 194 (2016) 169–201.

[15] J. Lee, U. von Gunten, J.H. Kim, Persulfate-based advanced oxidation: critical assessment of opportunities and roadblocks, Environ. Sci. Technol. 54 (2020) 3064–3081.

[16] Y.F. Ji, C. Ferronato, A. Salvador, X. Yang, J.M. Chovelon, Degradation of ciprofloxacin and sulfamethoxazole by ferrous-activated persulfate: Implications for remediation of groundwater contaminated by antibiotics, Sci. Total Environ. 472 (2014) 800–808.

[17] N. Chen, G.D. Fang, C.Y. Zhu, S. Wu, G.X. Liu, D.D. Dionysiou, X.L. Wang, J. Gao, D.M. Zhou, Surface-bound radical control rapid organic contaminant degradation through peroxymonosulfate activation by reduced Fe-bearing smectite clays, J. Hazard. Mater. 389 (2020), 121819.

[18] H.D. Xu, Y.Q. Sheng, New insights into the degradation of chloramphenicol and fluoroquinolone antibiotics by peroxymonosulfate activated with FeS: Performance and mechanism, Chem. Eng. J. 414 (2021), 128823.

[19] C.Q. Tan, X.C. Jian, Y.J. Dong, X. Lu, X.Y. Liu, H.M. Xiang, X.X. Cui, J. Deng, H. Y. Gao, Activation of peroxymonosulfate by a novel EGCE@$Fe_3O_4$ nanocomposite: Free radical reactions and implication for the degradation of sulfadiazine, Chem. Eng. J. 359 (2019) 594–603.

[20] J. Li, Y.J. Wan, Y.J. Li, G. Yao, B. Lai, Surface Fe(III)/Fe(II) cycle promoted the degradation of atrazine by peroxymonosulfate activation in the presence of hydroxylamine, Appl. Catal. B Environ. 256 (2019), 117782.

[21] H.H. Liu, J. Zhao, Y. Wang, Y.L. Wu, W.B. Dong, M.H. Nie, X.M. Wang, Enhancement of peroxymonosulfate activation by sinapic acid accelerating Fe(III)/Fe(II) cycle, Chem. Eng. J. 446 (2022), 137177.

[22] N.A. Mustapha, H. Liu, A.O. Ibrahim, Y. Huang, S. Liu, Degradation of aniline in groundwater by persulfate with natural subsurface sediment as the activator, Chem. Eng. J. 417 (2021), 128078.

[23] K.S. Sra, N.R. Thomson, J.F. Barker, Persistence of persulfate in uncontaminated aquifer materials, Environ. Sci. Technol. 44 (2010) 3098–3104.

[24] H.Z. Liu, T.A. Bruton, W. Li, J. Van Buren, C. Prasse, F.M. Doyle, D.L. Sedlak, Oxidation of benzene by persulfate in the presence of Fe(III)- and Mn(IV)-containing oxides: stoichiometric efficiency and transformation products, Environ. Sci. Technol. 50 (2016) 890–898.

[25] M. Tong, S.H. Yuan, S.C. Ma, M.G. Jin, D. Liu, D. Cheng, X.X. Liu, Y.Q. Gan, Y. X. Wang, Production of abundant hydroxyl radicals from oxygenation of subsurface sediments, Environ. Sci. Technol. 50 (2016) 214–221.

[26] W. Xie, S. Yuan, M. Tong, S. Ma, W. Liao, N.a. Zhang, C. Chen, Contaminant degradation by •OH during sediment oxygenation: dependence on Fe(II) species, Environ. Sci. Technol. 54 (5) (2020) 2975–2984.

[27] N. Chen, D.Y. Huang, G.X. Liu, L.G. Chu, G.D. Fang, C.Y. Zhu, D.M. Zhou, J. Gao, Active iron species driven hydroxyl radicals formation in oxygenation of different paddy soils: implications to polycyclic aromatic hydrocarbons degradation, Water Res. 203 (2021), 117484.

[28] N. Chen, Q.L. Fu, T.L. Wu, P.X. Cui, G.D. Fang, C. Liu, C.M. Chen, G.X. Liu, W. C. Wang, D.X. Wang, P. Wang, D.M. Zhou, Active iron phases regulate the abiotic transformation of organic carbon during redox fluctuation cycles of paddy Soil, Environ. Sci. Technol. 55 (2021) 14281–14293.

[29] O.S. Furman, A.L. Teel, R.J. Watts, Mechanism of base activation of persulfate, Environ. Sci. Technol. 44 (2010) 6423–6428.

[30] Y. Bai, E. Subdiaga, S.B. Haderlein, H. Knicker, A. Kappler, High-pH and anoxic conditions during soil organic matter extraction increases its electron-exchange capacity and ability to stimulate microbial Fe(III) reduction by electron shuttling, Biogeosciences 17 (2020) 683–698.

[31] E.E. Roden, A. Kappler, I. Bauer, J. Jiang, A. Paul, R. Stoesser, H. Konishi, H. Xu, Extracellular electron transfer through microbial reduction of solid-phase humic substances, Nat. Geosci. 3 (6) (2010) 417–421.

[32] J.E. Amonette, J.C. Templeton, Improvements to the quantitative assay of nonrefractory minerals for Fe(II) and total Fe using 1,10-phenanthroline, Clays Clay Miner. 46 (1998) 51–62.

[33] W.J. Liao, S.H. Yuan, X.X. Liu, M. Tong, Anoxic storage regenerates reactive Fe(II) in reduced nontronite with short-term oxidation, Geochim. Cosmochim. Acta 57 (2019) 96–109.

[34] H. Tamura, K. Goto, T. Yotsuyanagi, M. Nagayama, Spectrophotometric determination of iron (II) with 1,10-phenanthroline in the presence of large amounts of iron(III), Talanta 21 (4) (1974) 314–318.

[35] G. Heron, C. Crouzet, A.C.M. Bourg, T.H. Christensen, Speciation of Fe(II) and Fe (III) in contaminated aquifer sediments using chemical extraction techniques, Environ. Sci. Technol. 28 (1994) 1698–1750.

[36] A. Neumann, T.L. Olson, M.M. Scherer, Spectroscopic Evidence for Fe(II)–Fe(III) electron transfer at clay mineral edge and basal sites, Environ. Sci. Technol. 47 (2013) 6969–6977.

[37] B.J. Shi, K. Liu, L.L. Wu, W.Q. Li, C.M. Smeaton, B.L. Beard, C.M. Johnson, E. E. Roden, P. Van Cappellen, Iron isotope fractionations reveal a finite bioavailable Fe pool for structural Fe(III) reduction in nontronite, Environ. Sci. Technol. 50 (2016) 8661–8669.

[38] R.B. Garry, Spin trapping: ESR parameters of spin adducts, Free Radical Biol. Med. 3 (1987) 259–303.

[39] G.D. Fang, X.R. Chen, W.H. Wu, C. Liu, D.D. Dionysiou, T.T. Fan, Y.J. Wang, C. Y. Zhu, D.M. Zhou, Mechanisms of interaction between persulfate and soil constituents: activation, free radical formation, conversion and identification, Environ. Sci. Technol. 52 (2018) 14352–14361.

[40] Z. Wang, J. Wang, B. Xiong, F. Bai, S. Wang, Y. Wan, L.i. Zhang, P. Xie, M. R. Wiesner, Application of cobalt/peracetic acid to degrade sulfamethoxazole at neutral condition: efficiency and mechanisms, Environ. Sci. Technol. 54 (1) (2020) 464–475.

[41] F.Q. Liu, Z.J. Wang, S.J. You, Y.B. Liu, Electrogenerated quinone intermediates mediated peroxymonosulfate activation toward effective water decontamination and electrode antifouling, Appl. Catal. B: Environ. 320 (2023), 121980.

[42] X.X. Liu, S.H. Yuan, M. Tong, D. Liu, Oxidation of trichloroethylene by the hydroxyl radicals produced from oxygenation of reduced nontronite, Water Res. 113 (2017) 72–79.

[43] C.J. Liang, H.-W. Su, Identification of sulfate and hydroxyl radicals in thermally activated persulfate, Ind. Eng. Chem. Res. 48 (2009) 5558–5562.

[44] R.C. Zhang, P.Z. Sun, T.H. Boyer, L. Zhao, C.H. Huang, Degradation of pharmaceuticals and metabolite in synthetic human urine by UV, UV/$H_2O_2$, and UV/PDS, Environ. Sci. Technol. 49 (2015) 3056–3066.

[45] S. Gokulakrishnan, A. Mohammed, H. Prakash, Determination of persulphates using N, N-diethyl-p-phenylenediamine as colorimetric reagent: Oxidative coloration and degradation of the reagent without bactericidal effect in water, Chem. Eng. J. 286 (2016) 223–231.

[46] D. Dionysiou, G.P. Anipsitakis, Radical generation by the interaction of transition metals with common oxidants, Environ. Sci. Technol. 38 (2004) 3705–3712.

[47] H. Eibenberger, S. Steenken, P. O'Neill, D. Schulte-Frohlinde, Pulse radiolysis and electron spin resonance studies concerning the reaction of $SO_4^{\bullet}$ with alcohols and ethers in aqueous solution, J. Phys. Chem. 82 (1978) 749–750.

[48] C.J. Liang, C.-F. Huang, N. Mohanty, R.M. Kurakalva, A rapid spectrophotometric determination of persulfate anion in ISCO, Chemosphere 73 (2008) 1540–1543.

[49] U. Piotr, The OH-radical-induced chain reactions of methanol with hydrogen peroxide and with peroxodisulfate, J. Chem. Soc., Perkin Trans. 2 (2) (1997) 165–168.

[50] J. Liang, X.Y. Xu, Q.J. Zhong, Z.B. Xu, L. Zhao, H. Qiu, X.D. Cao, Roles of the mineral constituents in sludge-derived biochar in persulfate activation for phenol degradation, J. Hazard. Mater. 398 (2020), 122861.

[51] S.H. Yuan, X.X. Liu, W.J. Liao, P. Zhang, X.M. Wang, M. Tong, Mechanisms of electron transfer from structrual Fe(II) in reduced nontronite to oxygen for production of hydroxyl radicals, Geochim. Cosmochim. Acta 223 (2018) 422–436.

[52] J.F. Yan, J.L. Peng, L.D. Lai, F.Z. Ji, Y.H. Zhang, B. Lai, Q.X. Chen, G. Yao, X. Chen, L.P. Song, Activation $CuFe_2O_4$ by hydroxylamine for oxidation of antibiotic sulfamethoxazole, Environ. Sci. Technol. 52 (2018) 14302–14310.

[53] J.C. Li, L. Zhao, C.H. Huang, H.C. Zhang, R.C. Zhang, S. Elahi, P.Z. Sun, Significant effect of evaporation process on the reaction of sulfamethoxazole with manganese oxide, Environ. Sci. Technol. 54 (2020) 4856–4864.
[54] Z.J. Dong, C.C. Jiang, J.X. Yang, X. Zhang, W.L. Dai, P.W. Cai, Transformation of iodide by Fe(II) activated peroxydisulfate, J. Hazard. Mater. 373 (2019) 519–526.
[55] M. Zhang, X.Q. Chen, H. Zhou, M. Murugananthan, Y.R. Zhang, Degradation of p-nitrophenol by heat and metal ions co-activated persulfate, Chem. Eng. J. 264 (2015) 39–47.
[56] S.A. Hussain, Ş. Demirci, G. Özbayoğlu, Zeta potential measurements on three clays from Turkey and effects of clays on coal flotation, J. Colloid Interface Sci. 184 (1996) 535–541.